ACS Medicinal Chemistry Letters

pubs.acs.org/acsmedchemlett Letter

# AuNP Pyrazolo[3,4-*d*]pyrimidine Nanosystem in Combination with Radiotherapy against Glioblastoma

Alessio Molinari, Giulia Iovenitti, Arianna Mancini, Giovanni Luca Gravina, Monia Chebbi, Maura Caruana, Giulia Vignaroli, Francesco Orofino, Enrico Rango, Adriano Angelucci, Elena Dreassi,* Silvia Schenone, and Maurizio Botta

Cite This: *ACS Med. Chem. Lett.* 2020, 11, 664−670 Read Online

ACCESS | Metrics & More | Article Recommendations | Supporting Information

**ABSTRACT:** Gold-nanoparticle (AuNP)-conjugated drugs represent a promising and innovative antitumor therapeutic approach. In our study, we describe the design, the synthesis, the preparation, and the characterization of AuNPs conjugated with the pyrazolo[3,4-*d*]pyrimidine derivative SI306, a c-Src inhibitor. AuNPs−SI306 showed a good loading efficacy (65%), optimal stability in polar media and in human plasma, and a suitable morphological profile: a $\zeta$-potential of −43.9 mV, a nanoparticle diameter of 48.6 nm, and a 0.441 PDI value. The antitumoral activity of AuNPs−SI306 was evaluated *in vitro* in the glioblastoma model, by the low-density growth assay, and also in combination with radiotherapy (RT). Results demonstrated that AuNPs had a basal radiosensitization ability and that AuNPs−SI306, when used in combination with RT, were more effective in inhibiting tumor cell growth with respect to AuNPs and free SI306.

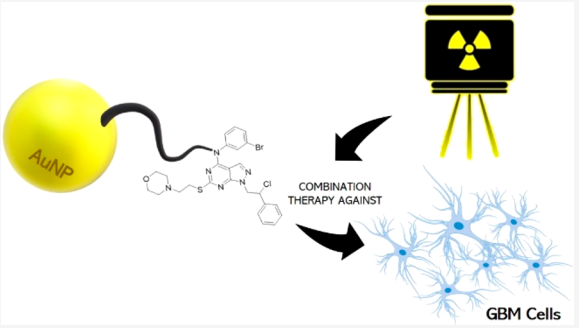


**KEYWORDS:** *Glioblastoma, Tyrosine kinase Src inhibitor, Nanotechnology, Gold nanoparticles, Radiotherapy*

Glioblastoma (GBM) is an aggressive intracranial tumor associated with high morbidity and mortality.[1] It is one of the most common brain tumors in adults and is characterized by a high growth rate, invasion, and demand for nutrients and oxygen, as demonstrated by frequent evidence of abundant microvascularity and necrosis.[2] Approximately 18% of reported brain tumors are GBM, with higher incidence in men.[3] The prognosis is very poor, with a median survival time expectancy of less than 1 year after the diagnosis and a 5 year survival rate of 5%, correlated with fatal relapse events.[4] The current standard treatment includes surgical resection followed by concomitant radiotherapy (RT) and temozolomide therapy, but these treatments are not able to improve the prognosis as desirable.[5] The major issues associated with therapeutic failure are represented by the selection of an effective molecular target and the penetration of the blood brain barrier (BBB).[6] For these reasons, novel therapeutic approaches are needed to improve the prognosis of GBM patients, which still remains an unmet medical need.

Aberrant regulation of tyrosine kinases (TKs) has been associated with different types of cancer, including GBM.[7] One of the most studied and promising targets in GBM is the protooncogene c-Src, a nonreceptor tyrosine kinase whose inhibition by several agents is currently being evaluated in the clinical phase. However, recent studies indicate that Src inhibitors, such as dasatinib and bosutinib, are ineffective as monotherapy in recurrent GBM.[8] The disappointing results obtained with monotherapy could be due to several factors, including the poor pharmacokinetics and tumor heterogeneity, but new effective drug combinations or innovative therapeutic formulations are being studies to increase the brain bioavailability and effectiveness also in association with RT.[9,10] Regardless of these results, c-Src remains a promising target based on its frequent upregulation in GBM tumor patients and its key role in promoting cancer invasion.[11,12]

In this context, nanomedicine seems to be the most versatile approach to design anticancer agent carriers, target delivery, and tumor imaging systems, with the aim to overcome poor biodistribution characteristics and therapeutic resistance issues.[13] New technologies based on nanometer-sized particles (nanotechnology) have been extensively investigated in the past decade, and this approach shows potential advantages for cancer diagnosis and treatment.[14] Nanometer-scale particles are able to better extravasate into brain tumor tissue due to the enhanced permeability and retention (EPR) effect, allowing a more efficient uptake of therapeutic molecules across the

**Special Issue:** In Memory of Maurizio Botta: His Vision of Medicinal Chemistry

**Received:** November 20, 2019
**Accepted:** March 5, 2020
**Published:** March 5, 2020





https://dx.doi.org/10.1021/acsmedchemlett.9b00538
*ACS Med. Chem. Lett.* 2020, 11, 664−670

BBB.[15] In particular, gold nanoparticles (AuNPs) have recently received much attention as a potential tool in cancer treatment and diagnosis due to their low toxicity,[16] ideal contrast agent properties for molecular computed tomography imaging, unique X-ray attenuation properties,[17] possibility of functionalization with various chemotherapeutic agents[18] or targeting ligands, and ability to enhance the efficacy of RT *in vitro* and *in vivo*.[19] Several clinical trials are being actively carried out for the approval of AuNPs for cancer diagnostics and therapy. An example is Aurimune (CYT-6091), AuNPs used as a vehicle for the delivery of recombinant human tumor necrosis factor alpha (rhTNF) into tumors.[20] Successful AuNP-mediated RT therapy studies against GBM have been reported by several research groups, highlighting an improved tumor response thanks to the enhanced tumor biodistribution of payload chemotherapeutics, radiation-induced BBB disruption, and increase in tumor perfusion reducing the hypoxic fraction of tumors.[21−23]

Pyrazolo[3,4-*d*]pyrimidine derivatives, a promising class of c-Src TK inhibitors[24] have been extensively studied by our research group. They exhibited strong antiproliferative and pro-apoptotic effects toward several cancer cell lines, including neuroblastoma,[25,26] chronic myeloid leukemia,[27] and GBM.[28] In particular, compound SI306 has shown a very good activity profile against GBM, alone or in combination with RT, both *in vitro* toward the U87 cell line and *in vivo* in both subcutaneous and intracranial GBM (U87 cells) models. SI306 was able to reduce the tumor mass volume by 40% when used alone and by 80% in combination with RT.[28] Nevertheless, the good antitumor activity of these promising compounds is usually associated with suboptimal aqueous solubility, which might hinder their further development. Recently, a prodrug strategy was applied with the aim of validating a novel and useful approach to overcome the poor aqueous solubility that characterizes this class of compounds.[29] The prodrug approach we developed was successful in improving the *in vitro* physicochemical and *in vivo* pharmacokinetic properties of SI306, thus allowing the parent drug as well as its prodrug to efficiently reach the brain.

To develop the prodrug design, we followed three steps: First, the most suitable position of the pyrazolo[3,4-*d*]-pyrimidine core to attach the prodrug linker was selected. Then, the appropriate enzymatically cleavable linker and solubilizing moiety were chosen. To design the most versatile protocol, the secondary amine in the C4 position was selected (Figure 1). Indeed, the NH group on the C4 position represents an essential feature to create favorable interactions

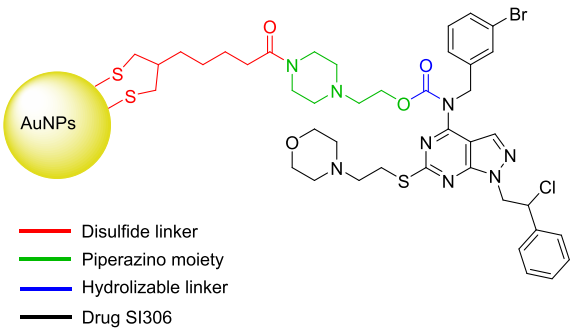


**Figure 1.** Structure of SI306 and the different portions of the AuNPs−SI306 nanosystem.

within the ATP binding site of TKs, as previously demonstrated by structure−activity relationships (SARs) and computational studies.[30] A thorough literature review suggested the O-alkyl carbamate moiety, easily cleavable *in vivo* by plasma esterases, as a viable linker to connect the secondary amino group at C4 with the solubilizing group.[31,32] Taking the water solubility issue into account, an *N*-methylpiperazino moiety, protonated at physiological pH ($pK_a$ 9.27 ± 0.1)[33] and characterized by a high water solubility (molar solubility 9.98 mol·L$^{-1}$, pH 7), was chosen to increase the water affinity of the prodrug in comparison with the starting drugs.

Starting from these assumptions, in this work, pyrazolo[3,4-*d*]pyrimidine-functionalized gold nanoparticles (AuNPs−SI306 nanosystem) were designed and synthesized as a potential agent for GBM treatment. After that, the AuNPs−SI306 nanosystem was characterized and tested alone and in combination with RT on the U87 GBM cell line (low-density growth assay), highlighting promising results compared with free SI306 and providing a novel effective nanotechnology to be potentially used against this malignancy.

The AuNPs−SI306 nanosystem is constituted by different portions, each designed to perform a determined function (Figure 1): the pyrazolo-pyrimidine core (black), which is the drug active against c-Src, AuNPs (yellow), which have been demonstrated to be able to increase the efficacy of RT, and a hydrolyzable linker (blue) that connects the drug and AuNPs and that is required to allow the drug release at the tumor site. On the basis of our experience in this field,[28] the O-alkyl carbamate could be a suitable *in vivo* hydrolyzable group to connect the secondary amine at C4 of the SI306 with the AuNPs. The drug would then be released by enzymatic hydrolysis to carry on its inhibitory activity, alone or in combination with RT. The piperazino moiety (green) was chosen for its solubility properties while also guaranteeing the possibility of performing a one-pot two-step synthetic approach (see later). To connect the piperazino moiety and the AuNPs, another link portion is necessary. The selection of the linker was based on two main aspects: first, the necessity of having a disulfide bridge, required to bind the AuNPs, and second, the availability of a moiety able to link the amino group of the piperazine. On the basis of the literature, the $\alpha$-lipoic acid (red) is a common stabilizing agent and linker used for the functionalization of AuNPs given the high affinity between sulfur (S) and gold (Au). Consequently, $\alpha$-lipoic acid was chosen as the most suitable linker to connect the drug to the AuNPs.[31]

The synthesis and characterization of pyrazolo[3,4-*d*]-pyrimidine compound SI306 were previously reported by us.[12] First of all, the synthetic approach to prepare the SI306-linker/hydrolyzable function derivative (**5**) was set up and developed in good yield, as summarized in Scheme 1.

Linker **2** was synthesized by a coupling reaction between the $\alpha$-lipoic acid and 1-(2-hydroxyethyl)piperazine using HOBt and EDC as activating agents. The preparation of **5** was performed by applying the one-pot, two-step synthetic approach previously developed in our laboratory.[29] The reaction of compound **3** (SI306) with triphosgene generated intermediate **4**, bearing the carbonyl-chloride group on the secondary amine at C4. The displacement of the chlorine using the appropriate alcohol (linker **2**) afforded the final product **5**.

Different methodologies for preparing AuNPs are widely reported in the literature[33−36] and provide the use of different


https://dx.doi.org/10.1021/acsmedchemlett.9b00538
ACS Med. Chem. Lett. 2020, 11, 664−670

**Scheme 1. Preparation of SI306-Linker/Hydrolyzable Function**[a]

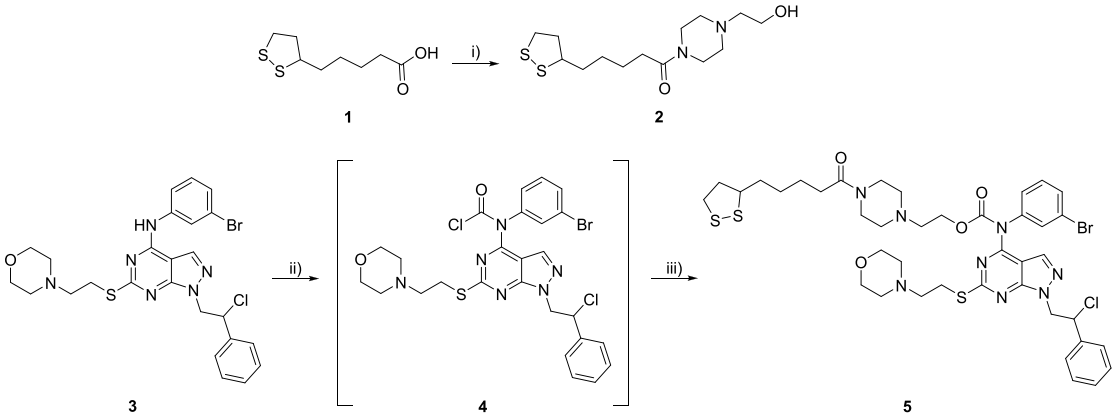


[a]Reagents and Conditions: (i) 1-(2-hydroxyethyl)piperazine, HOBt, EDC·HCl, $CH_2Cl_2$, rt, 12 h. (ii) $NaHCO_3$, triphosgene, $CH_2Cl_2$ dry, from 0 °C to rt, 6 h. (iii) Linker **2**, $CH_2Cl_2$ dry, rt, 72 h.

procedures and reagents. For our purpose, the Turkevich and Frens method[37] was chosen because of its compatibility with the pyrazolo[3,4-*d*]pyrimidine core (Scheme 2; see the Supporting Information for details).

**Scheme 2. Preparation of AuNPs**

$$HAuCl_4 \cdot 3H_2O + Na_3C_6H_5O_7 \cdot 2H_2O \xrightarrow{H_2O\ \text{milli-Q}} \text{AuNPs}$$

Other techniques that involve the use of $NaBH_4$ as a reducing agent were, in fact, not compatible with our molecules. On the contrary, the procedure we used encompassed the use of water as the solvent and trisodium citrate as the reducing and stabilizing agent. Furthermore, the selected procedure allowed the preparation of AuNPs with the right size (<30 nm).

Next, the following reaction of functionalization was performed in $H_2O$/DMSO 90:10 to guarantee the disulfide bridge formation between AuNPs and **5**.

Finally, to eliminate and quantify the unbound **5**, the AuNP suspension was ultracentrifugated (Beckman Coulter Optima L-90K; see the Supporting Information for details); after three ultracentrifugation cycles, the AuNPs−SI306 pellet was resuspended in water. The concentration of the compound in the supernatant solution was determined by LC-UV/MS, and the amount of AuNP-bound **5** was determined by the difference between the total amount of initial **5** added and the amount of **5** in the supernatants obtained during the purification step. (LC-UV/MS methods are reported in the Supporting Information.) Results showed a good loading efficacy % (LE%) with a value of 65%. (For details, see the Supporting Information.)

The successful functionalization was further confirmed by spectrophotometric UV−vis analysis (Figure 2): A red shift of ∼3 nm[37] of the maximum absorption wavelength between AuNPs (530.78 nm) and the AuNPs−SI306 nanosystem (533.01 nm) was recorded. In addition, usually, an absorption maximum around 530 nm indicates a nanoparticle size of 40 nm.[38] Moreover, the absence of peaks for high wavelengths suggested that no agglomeration of particles takes place under normal conditions.

Once the LE% was determined, bare AuNPs and AuNPs−SI306 nanosystems were characterized for mean diameter,

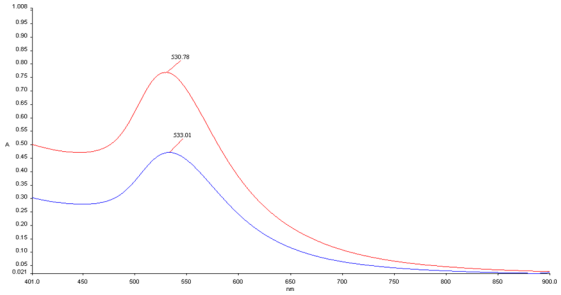


**Figure 2.** Spectrophotometric analysis in the UV−vis range (900−400 nm) of AuNPs (red line) and the AuNPs−SI306 nanosystem (blue line).

PDI, and ζ-potential (*Z*-pot.) by dynamic light scattering (DLS, Zeta Sizer Nano ZS90, Malvern Instruments, Malvern, U.K.). Nanoparticles were dispersed in water and measured at 24 °C with a scattering angle of 90°. The particle diameter should be in the 50−70 nm range to enhance the diffusion and transport through the BBB and allow the nanosystem to reach the brain,[39] improving the tumor penetration and retention.[40] Moreover, this diameter range strengthens the radiosensitization effects of AuNPs.[20]

The *Z*-pot. is a stability indicator and offers a prediction about the tendency of nanoparticles to form aggregates over time: Values greater than +25 mV or less than −25 mV are considered to be ideal.[22]

DLS measurements showed optimal results for the AuNPs−SI306 nanosystem, with no remarkable differences from bare AuNPs and revealing size and *Z*-pot. values of 48.6 nm and −43.9 mV, respectively. Moreover, the PDI value of 0.441 demonstrated a relatively monodispersed particle population (Table 1). These results suggest that the obtained nanosystem could represent a promising anti-GBM platform, especially in association with RT.[41−43]

To probe the nanoparticle agglomeration state in the presence of salts and proteins, UV−vis spectra have been recorded upon the addition of NaCl or KCl (0.01 to 0.1 M concentration range) or human serum albumin (HSA, 12.5, 25, 50 mg/mL) to the AuNP suspension. HSA and salts at lower concentration did not affect the stability of AuNPs, and no agglomeration took place. On the contrary, AuNPs showed a visible color change from red to blue (example in Figure 3B,C)


https://dx.doi.org/10.1021/acsmedchemlett.9b00538
ACS Med. Chem. Lett. 2020, 11, 664−670

**Table 1. DLS Characterization of AuNPs−SI306 and Bare AuNPs[a]**

| sample | Z-pot. (mV) | size (nm) | PDI |
|---|---|---|---|
| AuNPs−SI306 | −43.9 ± 0.4 | 48.6 ± 1.3 | 0.441 ± 0.02 |
| bare AuNPs | −41.5 ± 1.1 | 41.8 ± 0.9 | 0.637 ± 0.05 |

[a]Mean values ± S.D. calculated from three independent experiments ($n$ = 3). For experimental details, see the Supporting Information.

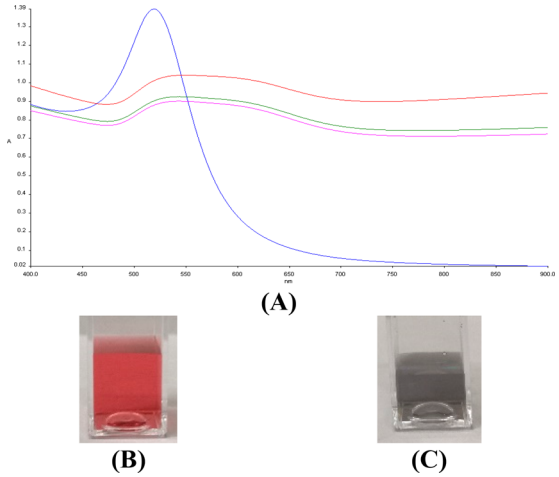


**Figure 3.** (A) Time-resolved UV−vis spectra of AuNPs (blue) and AuNPs upon interaction with NaCl 0.1 M after 1 (red), 5 (green), and 10 min (pink). (B) Aspect of AuNPs. (C) Aspect of AuNPs immediately after NaCl 0.1 M addition.

upon the addition of salts at higher concentrations due to the formation of aggregates, also highlighted by a red shift and broadening of the surface plasmon band, as in Figure 3A, which shows the spectrum of AuNPs upon the addition of NaCl 0.1 M. (For more details, see the Supporting Information.)

To avoid potential side effects as well as guarantee the highest efficacy, the active compound SI306 should be released from the AuNPs−SI306 nanosystem. To investigate this aspect, the rate of plasma hydrolysis was evaluated *in vitro*. First, the stability in polar media such as $H_2O$, ACN, methanol, DMSO, and PBS was evaluated by LC-UV/MS. The determined half-lives ($t_{1/2}$) resulted in being>48 h, confirming the good stability of the AuNPs−SI306 nanosystem. This good stability allowed us to run the subsequent studies. The nanosystem was then incubated in human plasma at 37 °C, and the release rate of SI306 was monitored by LC-UV/MS at different time points over 24 h. As expected, good plasma hydrolysis of the carbamate linker after 24 h was found (76%), indicating the release of the antitumor compound by plasma esterases via enzymatic hydrolysis.

Figure 4 shows the antiproliferative effects of the AuNPs−SI306 nanosystem, the respective nonfunctionalized AuNPs, and the free SI306 dissolved in DMSO evaluated alone (orange bars) and in combination with RT (blue bars) at two different final concentrations of SI306 (1 and 10 $\mu$M) by cell low-density growth assay using the U87 GBM cell line.[12] (For materials and methods, see the Supporting Information.) In Table 2, the reduction in cell viability % with respect to the corresponding control (vehicle-associated or not with RT, CNTRL) has been reported for all of the tested formulations.

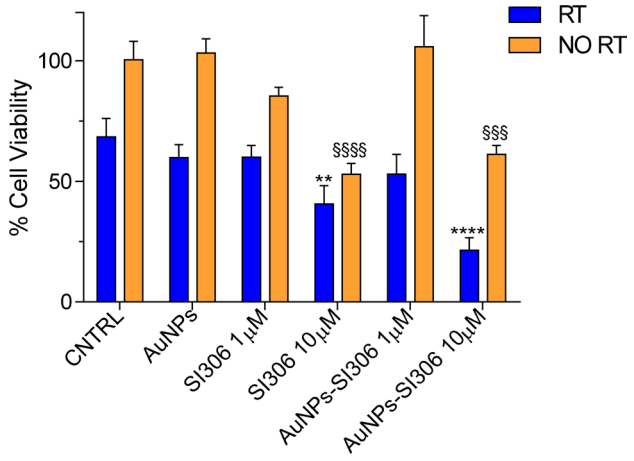


**Figure 4.** *In vitro* antiproliferative effect of AuNPs, SI306, and the AuNPs−SI306 nanosystem. Results are expressed as the percentage mean ± SD ($n$ = 3). A Bonferroni's one-way multiple comparisons test (ANOVA) was performed to test the significance of the observed differences. * indicates statistically significant differences in group "RT" (blue bars) versus CNTRL RT (**$p$ < 0.01, ****$p$ < 0.0001). § indicates statistically significant differences in group "NO RT" (orange bars) versus CNTRL NO RT ($^{§§§}p$ < 0.001, $^{§§§§}p$ < 0.0001).

**Table 2. Mean Reduction % in Cell Viability ± S.D. with Respect to Corresponding CNTRL (RT or NO RT)[a]**

| samples | RT | NO RT |
|---|---|---|
| AuNPs | 12.60 ± 7.88 | 0 |
| SI306 1 $\mu$M | 12.35 ± 7.23 | 14.96 ± 3.60 |
| SI306 10 $\mu$M | 40.62 ± 11.07 | 47.32 ± 4.47 |
| AuNPs−SI306 1 $\mu$M | 22.57 ± 12.07** | 0 |
| AuNPs−SI306 10 $\mu$M | 68.65 ± 7.51*** | 39.02 ± 3.68 |

[a]Bonferroni's one-way multiple comparisons test (ANOVA) was performed. Asterisks mark significantly different values between RT and NO RT in the row. **, $p$ < 0.01. ***, $p$ < 0.001.

As expected, nonfunctionalized AuNPs, when not associated with RT, did not provoke any mortality in cells, proving to be safe. In addition, nonirradiated cell growth was inhibited exclusively by free SI306 (10 $\mu$M) and AuNPs−SI306 (10 $\mu$M). However, because nonfunctionalized AuNPs did not show any effect, it is likely that the inhibitory activity of AuNPs−SI306 is due to the SI306 portion and not to AuNP system. On the contrary, when combined with RT, nonfunctionalized AuNPs were able to slightly reduce the proliferation of U87 cells with respect to their corresponding control (~13% reduction). Free SI306 has been proved to be active in reducing the GBM cell viability, but RT did not enhance its antiproliferative effect. Indeed, from the statistical analysis reported in Table 2, significant differences between free SI306 with or without RT have not been observed for either 1 (12 and 15%, respectively) or 10 $\mu$M (40 and 47%, respectively) concentration. However, the highest antiproliferative effect was achieved by the combination treatment with the AuNPs−SI306 nanosystem (10 $\mu$M) and RT. This combination resulted in a significant decrease in the number of viable cells of ~70% with respect to RT alone.

In conclusion, in this work, we have reported the design, preparation, and characterization of the AuNPs−SI306 nanosystem as a novel potential anticancer agent toward GBM. AuNPs were prepared using the Turkevich and Frens method, whereas the key compound **5** was synthesized in good yield by


https://dx.doi.org/10.1021/acsmedchemlett.9b00538
ACS Med. Chem. Lett. 2020, 11, 664−670

exploiting a one-pot, two-step approach developed in our laboratories.

The functionalization of AuNPs with compound **5** was achieved (qualitatively confirmed by spectrophotometric analysis) with a 65% loading efficacy (quantitatively confirmed by LC-UV/MS analysis) after the disulfide bridge formation between AuNPs and **5**. The characterization of the nanosystem showed an optimal stability and morphology profile: $t_{1/2}$ in polar media >48 h, release of 76% of the active compound SI306 when incubated with human plasma, *Z*-pot. of −43.9 mV, nanoparticle diameter of 48.6 nm, and 0.441 PDI value. Moreover, a biological assay with the U87 cell line has proved an effective antiproliferative activity of the association between the AuNPs−SI306 nanosystem and RT that was significantly higher than the effect of SI306, AuNPs, and RT alone.

Taken together, the results described in this work reflect the promising properties of the molecule SI306 when developed as a AuNP nanosystem toward GBM. This strategy might allow us not only to exploit the synergy of RT with both a gold platform and the pyrazolo[3,4-*d*]pyrimidine compound but also to overcome the problems related to tumor localization and the pharmacokinetic issues related to the poor solubility of SI306.

Our results offer a promising rationale for the further development of the AuNPs−SI306 nanosystem and for experimental confirmation in different cancer models.

## ■ ASSOCIATED CONTENT

### Supporting Information

The Supporting Information is available free of charge at https://pubs.acs.org/doi/10.1021/acsmedchemlett.9b00538.

Reagents and instruments, synthetic procedures, NMR and LC−MS characterization, preparation and characterization of AuNPs and AuNPs−SI306, and biological assay (PDF)

## ■ AUTHOR INFORMATION


### Corresponding Author

**Elena Dreassi** − *Dipartimento Biotecnologie, Chimica e Farmacia, Università degli Studi di Siena, 53100 Siena, Italy;* orcid.org/0000-0001-8987-940X; Phone: +39-0577 234321; Email: elena.dreassi@unisi.it

### Authors

**Alessio Molinari** − *Dipartimento Biotecnologie, Chimica e Farmacia, Università degli Studi di Siena, 53100 Siena, Italy*

**Giulia Iovenitti** − *Dipartimento Biotecnologie, Chimica e Farmacia, Università degli Studi di Siena, 53100 Siena, Italy*

**Arianna Mancini** − *Dipartimento Biotecnologie, Chimica e Farmacia, Università degli Studi di Siena, 53100 Siena, Italy; Dipartimento di Farmacia, Università di Pisa, 56126 Pisa, Italy*

**Giovanni Luca Gravina** − *Dipartimento di Scienze Cliniche Applicate e Biotecnologiche, Università dell'Aquila, 67100 Aquila, Coppito, Italy*

**Monia Chebbi** − *Dipartimento Biotecnologie, Chimica e Farmacia, Università degli Studi di Siena, 53100 Siena, Italy; Faculty of Sciences, Laboratory of Physical Chemistry of Condensed Materials, University of Tunis El Manar, 2092 Tunis, Tunisia*

**Maura Caruana** − *Dipartimento Biotecnologie, Chimica e Farmacia, Università degli Studi di Siena, 53100 Siena, Italy*

**Giulia Vignaroli** − *Dipartimento Biotecnologie, Chimica e Farmacia, Università degli Studi di Siena, 53100 Siena, Italy*

**Francesco Orofino** − *Dipartimento Biotecnologie, Chimica e Farmacia, Università degli Studi di Siena, 53100 Siena, Italy*

**Enrico Rango** − *Dipartimento Biotecnologie, Chimica e Farmacia, Università degli Studi di Siena, 53100 Siena, Italy*

**Adriano Angelucci** − *Dipartimento di Scienze Cliniche Applicate e Biotecnologiche, Università dell'Aquila, 67100 Aquila, Coppito, Italy;* orcid.org/0000-0002-8755-1889

**Silvia Schenone** − *Dipartimento di Scienze Farmaceutiche, Università degli Studi di Genova, 16132 Genova, Italy*

○**Maurizio Botta** − *Dipartimento Biotecnologie, Chimica e Farmacia, Università degli Studi di Siena, 53100 Siena, Italy; Lead Discovery Siena S.r.l., 53019 Siena, Italy; Sbarro Institute for Cancer Research and Molecular Medicine, Center for Biotechnology, College of Science and Technology, Temple University, Philadelphia, Pennsylvania 19122, United States;* orcid.org/0000-0003-0456-6995

Complete contact information is available at: https://pubs.acs.org/10.1021/acsmedchemlett.9b00538


### Author Contributions

Conceptualization: A. Molinari, G.V., S.S., and M.B.; synthesis methodology and characterization: A. Molinari, G.I., M. Chebbi, M. Caruana, and F.O.; analysis and characterization of NPs: G.I., A. Mancini, E.R., and E.D.; biological assays: G.L.G. and A.A.; draft preparation and formatting: G.I., A. Mancini, E.R., A.A., and E.D.; supervision: G.V., E.D., S.S., and M.B. All authors have given approval to the final version of the manuscript.

### Notes

The authors declare no competing financial interest.

○Deceased on August 2, 2019.

## ■ ACKNOWLEDGMENTS

The work was supported in part by AIRC (Associazione Italiana per la Ricerca sul Cancro) grant IG-2015, code 17677.

## ■ DEDICATION

This paper is dedicated to the memory of Professor Maurizio Botta.

## ■ ABBREVIATIONS

AuNP, gold nanoparticle; GBM, glioblastoma; PDI, polydispersity index; RT, radiotherapy; BBB, blood brain barrier; TK, tyrosine kinase; EPR, enhanced permeability and retention; rhTNF, recombinant human tumor necrosis factor alpha; SAR, structure−activity relationship; HOBt, 1-hydroxybenzotriazole hydrate; EDC, *N*-(3-(dimethylamino)propyl)-*N*′-ethylcarbodiimide; LE%, loading efficacy %; *Z*-pot., $\zeta$ potential; DLS, dynamic light scattering; $t_{1/2}$, half life; ACN, acetonitrile; DMSO, dimethyl sulfoxide; PBS, phosphate buffered saline; CNTRL, control; NO RT, no radiotherapy

## ■ REFERENCES


(1) Furnari, F. B.; Fenton, T.; Bachoo, R. M.; Mukasa, A.; Stommel, J. M.; Stegh, A.; Hahn, W. C.; Ligon, K. L.; Louis, D. N.; Brennan, C.; et al. Malignant Astrocytic Glioma: Genetics, Biology, and Paths to Treatment. *Genes Dev.* **2007**, *21*, 2683−2710.

(2) Wen, P. Y.; Kesari, S. Malignant Gliomas in Adults. *N. Engl. J. Med.* **2008**, *359*, 492−507.

(3) Tamimi, A. F.; Juweid, M. Epidemiology and Outcome of Glioblastoma. *Glioblastoma* **2017**, 143−153.
(4) Jhanwar-Uniyal, M.; Labagnara, M.; Friedman, M.; Kwasnicki, A.; Murali, R. Glioblastoma: Molecular Pathways. *Cancers* **2015**, *7*, 538−555.
(5) Stupp, R.; Mason, W. P.; Van Den Bent, M. J.; Weller, M.; Fisher, B.; Taphoorn, M. J. B.; Belanger, K.; Brandes, A. A.; Marosi, C.; Bogdahn, U.; et al. Radiotherapy plus Concomitant and Adjuvant Temozolomide for Glioblastoma. *N. Engl. J. Med.* **2005**, *352*, 987−996.
(6) Ahluwalia, M. S.; de Groot, J.; Liu, W. M.; Gladson, C. L. Targeting SRC in Glioblastoma Tumors and Brain Metastases: Rationale and Preclinical Studies. *Cancer Lett.* **2010**, *298*, 139−149.
(7) Irby, R. B.; Yeatman, T. J. Role of Src Expression and Activation in Human Cancer. *Oncogene* **2000**, *19*, 5636−5642.
(8) Taylor, J. W.; Dietrich, J.; Gerstner, E. R.; Norden, A. D.; Rinne, M. L.; Cahill, D. P.; Stemmer-Rachamimov, A.; Wen, P. Y.; Betensky, R. A.; Giorgio, D. H.; et al. Phase 2 Study of Bosutinib, a Src Inhibitor, in Adults with Recurrent Glioblastoma. *J. Neuro-Oncol.* **2015**, *121*, 557−563.
(9) Alphandéry, E. Glioblastoma Treatments: An Account of Recent Industrial Developments. *Front. Pharmacol.* **2018**, *9*, 879.
(10) Nam, L.; Coll, C.; Erthal, L. C. S.; de la Torre, C.; Serrano, D.; Martínez-Máñez, R.; Santos-Martínez, M. J.; Ruiz-Hernández, E. Drug Delivery Nanosystems for the Localized Treatment of Glioblastoma Multiforme. *Materials* **2018**, *11*, No. 779.
(11) Bertram, J. S. The Molecular Biology of Cancer. *Mol. Aspects Med.* **2000**, *21*, 167−223.
(12) Calgani, A.; Vignaroli, G.; Zamperini, C.; Coniglio, F.; Festuccia, C.; Di Cesare, E.; Gravina, G. L.; Mattei, C.; Vitale, F.; Schenone, S.; et al. Suppression of SRC Signaling Is Effective in Reducing Synergy between Glioblastoma and Stromal Cells. *Mol. Cancer Ther.* **2016**, *15*, 1535−1544.
(13) Pillai, G. Nanomedicines for Cancer Therapy: An Update of FDA Approved and Those under Various Stages of Development. *SOJ. Pharm. Pharm. Sci.* **2014**, *1*, 13.
(14) Glaser, T.; Han, I.; Wu, L.; Zeng, X. Targeted Nanotechnology in Glioblastoma Multiforme. *Front. Pharmacol.* **2017**, *8*, 166.
(15) Cheng, Y.; Dai, Q.; Morshed, R. A.; Fan, X.; Wegscheid, M. L.; Wainwright, D. A.; Han, Y.; Zhang, L.; Auffinger, B.; Tobias, A. L.; Rincon, E.; Thaci, B.; Ahmed, A. U.; Warnke, P. C.; He, C.; Lesniak, M. S. Blood-brain barrier permeable gold nanoparticles: an efficient delivery platform for enhanced malignant glioma therapy and imaging. *Small* **2014**, *24*, 5137−5150.
(16) Connor, E. E.; Mwamuka, J.; Gole, A.; Murphy, C. J.; Wyatt, M. D. Gold Nanoparticles Are Taken up by Human Cells but Do Not Cause Acute Cytotoxicity. *Small* **2005**, *1*, 325−327.
(17) Popovtzer, R.; Agrawal, A.; Kotov, N. A.; Popovtzer, A.; Balter, J.; Carey, T. E.; Kopelman, R. Targeted Gold Nanoparticles Enable Molecular CT Imaging of Cancer. *Nano Lett.* **2008**, *8*, 4593−4596.
(18) Gibson, J. D.; Khanal, B. P.; Zubarev, E. R. Paclitaxel-Functionalized Gold Nanoparticles. *J. Am. Chem. Soc.* **2007**, *129*, 11653−11661.
(19) Liu, C. J.; Wang, C. H.; Chien, C. C.; Yang, T. Y.; Chen, S. T.; Leng, W. H.; Lee, C. F.; Lee, K. H.; Hwu, Y.; Lee, Y. C.; et al. Enhanced X-Ray Irradiation-Induced Cancer Cell Damage by Gold Nanoparticles Treated by a New Synthesis Method of Polyethylene Glycol Modification. *Nanotechnology* **2008**, *19*, 295104.
(20) Libutti, S. K.; Paciotti, G. F.; Byrnes, A. A.; Alexander, H. R.; Gannon, W. E.; Walker, M.; Seidel, G. D.; Yuldasheva, N.; Tamarkin, L. Phase I and Pharmacokinetic Studies of CYT-6091, a Novel PEGylated Colloidal Gold-RhTNF Nanomedicine. *Clin. Cancer Res.* **2010**, *16*, 6139−6149.
(21) Coluccia, D.; Figueiredo, C. A.; Wu, M. Y. J.; Riemenschneider, A. N.; Diaz, R.; Luck, A.; Smith, C.; Das, S.; Ackerley, C.; O'Reilly, M.; et al. Enhancing Glioblastoma Treatment Using Cisplatin-Gold-Nanoparticle Conjugates and Targeted Delivery with Magnetic Resonance-Guided Focused Ultrasound. *Nanomedicine* **2018**, *14*, 1137−1148.
(22) Joh, D. Y.; Sun, L.; Stangl, M.; Al Zaki, A.; Murty, S.; Santoiemma, P. P.; Davis, J. J.; Baumann, B. C.; Alonso-Basanta, M.; Bhang, D. Selective Targeting of Brain Tumors with Gold Nanoparticle-Induced Radiosensitization. *PLoS One* **2013**, *8*, e62425.
(23) Bouras, A.; Kaluzova, M.; Hadjipanayis, C. G. Radiosensitivity Enhancement of Radioresistant Glioblastoma by Epidermal Growth Factor Receptor Antibody-Conjugated Iron-Oxide Nanoparticles. *J. Neuro-Oncol.* **2015**, *124*, 13−22.
(24) Schenone, S.; Brullo, C.; Musumeci, F.; Botta, M. Novel Dual Src/Abl Inhibitors for Hematologic and Solid Malignancies. *Expert Opin. Invest. Drugs* **2010**, *19*, 931−945.
(25) Navarra, M.; Celano, M.; Maiuolo, J.; Schenone, S.; Botta, M.; Angelucci, A.; Bramanti, P.; Russo, D. Antiproliferative and Pro-Apoptotic Effects Afforded by Novel Src-Kinase Inhibitors in Human Neuroblastoma Cells. *BMC Cancer* **2010**, *10*, 602.
(26) Radi, M.; Brullo, C.; Crespan, E.; Tintori, C.; Musumeci, F.; Biava, M.; Schenone, S.; Dreassi, E.; Zamperini, C.; Maga, G.; et al. Identification of Potent C-Src Inhibitors Strongly Affecting the Proliferation of Human Neuroblastoma Cells. *Bioorg. Med. Chem. Lett.* **2011**, *21*, 5928−5933.
(27) Radi, M.; Tintori, C.; Musumeci, F.; Brullo, C.; Zamperini, C.; Dreassi, E.; Fallacara, A. L.; Vignaroli, G.; Crespan, E.; Zanoli, S.; et al. Design, Synthesis, and Biological Evaluation of Pyrazolo[3,4-d]Pyrimidines Active in Vivo on the Bcr-Abl T315I Mutant. *J. Med. Chem.* **2013**, *56*, 5382−5394.
(28) Ceccherini, E.; Indovina, P.; Zamperini, C.; Dreassi, E.; Casini, N.; Cutaia, O.; Forte, I. M.; Pentimalli, F.; Esposito, L.; Polito, M. S.; et al. SRC Family Kinase Inhibition through a New Pyrazolo[3,4-d]Pyrimidine Derivative as a Feasible Approach for Glioblastoma Treatment. *J. Cell. Biochem.* **2015**, *116*, 856−863.
(29) Vignaroli, G.; Iovenitti, G.; Zamperini, C.; Coniglio, F.; Calandro, P.; Molinari, A.; Fallacara, A. L.; Sartucci, A.; Calgani, A.; Colecchia, D.; et al. Prodrugs of Pyrazolo[3,4-*d*]Pyrimidines: From Library Synthesis to Evaluation as Potential Anticancer Agents in an Orthotopic Glioblastoma Model. *J. Med. Chem.* **2017**, *60*, 6305−6320.
(30) Tintori, C.; Magnani, M.; Schenone, S.; Botta, M. Docking, 3D-QSAR Studies and in Silico ADME Prediction on c-Src Tyrosine Kinase Inhibitors. *Eur. J. Med. Chem.* **2009**, *44*, 990−1000.
(31) Persson, G.; Pahlm, O.; gnosspelius, Y. Oral Bambuterol versus Terbutaline in Patients with Asthma. *Curr. Ther. Res.* **1995**, *56*, 457−465.
(32) Slatter, J. G.; Schaaf, L. J.; Sams, J. P.; Feenstra, K. L.; Johnson, M. G.; Bombardt, P. A.; Cathcart, K. S.; Verburg, M. T.; Pearson, L. K.; Compton, L. D.; et al. Pharmacokinetics, Metabolism, and Excretion of Irinotecan (CPT-11) Following i.v. Infusion of [14C]CPT-11 in Cancer Patients. *Drug Metab. Dispos.* **2000**, *28*, 423−433.
(33) Sillén, L. G.; Martell, A. E.; Bjerrum, J. Stability Constants of Metal-Ion Complexes. In *Stability Constants. Part I: Organic Ligands*; Special Publication No. *6*; Chemical Society: London, 1964.
(34) Lasic, D.; Papahadjopoulos, D. *Medical Applications of Liposomes*; Elsevier, 1998.
(35) Tintori, C.; Fallacara, A. L.; Radi, M.; Zamperini, C.; Dreassi, E.; Crespan, E.; Maga, G.; Schenone, S.; Musumeci, F.; Brullo, C.; et al. Combining X-Ray Crystallography and Molecular Modeling toward the Optimization of Pyrazolo[3,4-d]Pyrimidines as Potent c-Src Inhibitors Active in Vivo against Neuroblastoma. *J. Med. Chem.* **2015**, *58*, 347−361.
(36) Daniel, M. C.; Astruc, D. Gold Nanoparticles: Assembly, Supramolecular Chemistry, Quantum-Size-Related Properties, and Applications toward Biology, Catalysis, and Nanotechnology. *Chem. Rev.* **2004**, *104*, 293−346.
(37) Kimling, J.; Maier, M.; Okenve, B.; Kotaidis, V.; Ballot, H.; Plech, A. Turkevich Method for Gold Nanoparticle Synthesis Revisited. *J. Phys. Chem. B* **2006**, *110*, 15700−15707.
(38) He, Y. Q.; Liu, S. P.; Kong, L.; Liu, Z. F. A Study on the Sizes and Concentrations of Gold Nanoparticles by Spectra of Absorption, Resonance Rayleigh Scattering and Resonance Non-Linear Scattering. *Spectrochim. Acta, Part A* **2005**, *61*, 2861−2866.


https://dx.doi.org/10.1021/acsmedchemlett.9b00538
*ACS Med. Chem. Lett.* 2020, 11, 664−670

(39) Stiti, M.; Cecchi, A.; Rami, M.; Abdaoui, M.; Barragan-Montero, V.; Scozzafava, A.; Guari, Y.; Winum, J. Y.; Supuran, C. T. Carbonic Anhydrase Inhibitor Coated Gold Nanoparticles Selectively Inhibit the Tumor-Associated Lsoform IX over the Cytosolic Isozymes I and II. *J. Am. Chem. Soc.* **2008**, *130*, 16130−16131.
(40) Khan, A. K.; Rashid, R.; Murtaza, G.; Zahra, A. Gold Nanoparticles: Synthesis and Applications in Drug Delivery. *Trop. J. Pharm. Res.* **2014**, *13*, 1169−1177.
(41) Huo, S.; Ma, H.; Huang, K.; Liu, J.; Wei, T.; Jin, S.; Zhang, J.; He, S.; Liang, X. J. Superior Penetration and Retention Behavior of 50 Nm Gold Nanoparticles in Tumors. *Cancer Res.* **2013**, *73*, 319−330.
(42) Yamamoto, T.; Nakai, K.; Tsurubuchi, T.; Matsuda, M.; Shirakawa, M.; Zaboronok, A.; Endo, K.; Matsumura, A. Boron Neutron Capture Therapy for Newly Diagnosed Glioblastoma: A Pilot Study in Tsukuba. *Appl. Radiat. Isot.* **2009**, *67*, S25.
(43) Honary, S.; Zahir, F. Effect of Zeta Potential on the Properties of Nano-Drug Delivery Systems - A Review (Part 2). *Trop. J. Pharm. Res.* **2013**, *12*, 265−273.


https://dx.doi.org/10.1021/acsmedchemlett.9b00538
*ACS Med. Chem. Lett.* 2020, 11, 664−670